galaxies

MDPI

Review

X-ray Polarization of Blazars and Radio Galaxies Measured by the Imaging X-ray Polarimetry Explorer

Alan P. Marscher [1,*], Laura Di Gesu [2], Svetlana G. Jorstad [1,3], Dawoon E. Kim [4,5,6], Ioannis Liodakis [7,8], Riccardo Middei [9,10] and Fabrizio Tavecchio [11]

1 Institute for Astrophysical Research, Boston University, 725 Commonwealth Ave., Boston, MA 01225, USA; jorstad@bu.edu
2 ASI—Agenzia Spaziale Italiana, Via del Politecnico snc, 00133 Rome, Italy
3 Department of Astrophysics, St. Petersburg State University, 7/9, Universitetskaya nab., 199034 St. Petersburg, Russia
4 Italian National Institute for Astrophysics (INAF), Istituto di Astrofisica e Planetologia Spaziali, Via Fosso del Cavaliere 100, 00133 Rome, Italy; dawoon.kim@inaf.it
5 Dipartimento di Fisica, Università degli Studi di Roma "La Sapienza", Piazzale Aldo Moro 5, 00185 Rome, Italy
6 Dipartimento di Fisica, Università degli Studi di Roma "Tor Vergata", Via della Ricerca Scientifica 1, 00133 Rome, Italy
7 NASA Marshall Space Flight Center, Huntsville, AL 35812, USA
8 Institute of Astrophysics, Foundation for Research and Technology-Hellas, GR-70013 Heraklion, Greece
9 INAF Osservatorio Astronomico di Roma, Via Frascati 33, Monte Porzio Catone (RM), 00078 Rome, Italy
10 Space Science Data Center, Agenzia Spaziale Italiana, Via del Politecnico snc, 00133 Rome, Italy
11 INAF Osservatorio Astronomico di Brera, Via E. Bianchi 46, Merate (LC), 23807 Milan, Italy
* Correspondence: marscher@bu.edu

Abstract: X-ray polarization, which now can be measured by the Imaging X-ray Polarimetry Explorer (IXPE), is a new probe of jets in the supermassive black hole systems of active galactic nuclei (AGNs). Here, we summarize IXPE observations of radio-loud AGNs that have been published thus far. Blazars with synchrotron spectral energy distributions (SEDs) that peak at X-ray energies are routinely detected. The degree of X-ray polarization is considerably higher than at longer wavelengths. This is readily explained by energy stratification of the emission regions when electrons lose energy via radiation as they propagate away from the sites of particle acceleration as predicted in shock models. However, the 2–8 keV polarization electric vector is not always aligned with the jet direction as one would expect unless the shock is oblique. Magnetic reconnection may provide an alternative explanation. The rotation of the polarization vector in Mrk421 suggests the presence of a helical magnetic field in the jet. In blazars with lower-frequency peaks and the radio galaxy Centaurus A, the non-detection of X-ray polarization by IXPE constrains the X-ray emission mechanism.

Keywords: X-ray polarization; high-energy processes; astrophysical jets; black holes

Citation: Marscher, A.P.; Di Gesu, L.; Jorstad, S.G.; Kim, D.E.; Liodakis, I.; Middei, R.; Tavecchio, F. X-ray Polarization of Blazars and Radio Galaxies Measured by the Imaging X-ray Polarimetry Explorer. *Galaxies* **2024**, *12*, 50. https://doi.org/10.3390/galaxies12040050

Academic Editor: Alicja Wierzcholska

Received: 9 July 2024
Revised: 8 August 2024
Accepted: 15 August 2024
Published: 22 August 2024

1. Introduction

While all radio-loud active galactic nuclei (RLAGNs) exhibit luminous X-ray emission, there are multiple processes by which the X-rays might be produced. These include Compton scattering by hot electrons in the "corona" of the accretion disk near the central black hole [1], synchrotron radiation by high-energy electrons in a relativistic jet, Compton scattering of the synchrotron photons by the same electrons (synchrotron self-Compton, SSC; [2]), Compton scattering of photons from outside the jet by electrons in the jet (external Compton, EC [3]), proton synchrotron radiation, and synchrotron or Compton emission by particles produced by collisions of hadrons in the jet with photons [4]. The spectral energy distribution (SED; see Figure 1) provides one way of determining the dominant process in a given RLAGN: if the optical-uv portion of the SED can be smoothly connected

with the X-ray portion across the far-uv gap in observational data, synchrotron radiation by the highest-energy electrons is a prime candidate for the X-ray emission process. If the extension of the optical-uv SED falls below the X-ray flux, and the X-ray spectrum is flatter than at optical frequencies, Compton scattering or emission from relativistic protons could be dominant.

A second test of X-ray emission models became available starting in early 2022 when the orbiting Imaging X-ray Polarimetry Explorer (IXPE; [5]) began science operations. This takes advantage of different processes producing distinct polarization properties. IXPE is sensitive enough to measure the linear polarization of some X-ray bright RLAGNs. Thus far, it has detected polarization above the 99% significance level (MDP99; [6]) in half a dozen BL Lacertae objects (see Table 1), all of whose SEDs exhibit a peak at X-ray energies (with a second peak at GeV γ-ray energies), termed "high-synchrotron-peaked" (HSP; [7]) blazars (see Figure 1). In these blazars, the emission of the lower-frequency portion of the SED has the properties of incoherent synchrotron radiation, with the X-rays being emitted by the highest-energy electrons produced in the relativistic jet. The polarization electric vector position angle (EVPA) in optically thin synchrotron radiation is perpendicular to the direction of the magnetic field of the emitting plasma as projected on the sky (after correction for relativistic aberration; [8]). The degree of polarization relative to the maximum value of 70–75% is a probe of the level of order of the magnetic field, with lower polarization corresponding to greater disorder [9].

Since the X-ray emission of HSP blazars is produced by the highest-energy electrons, which do not maintain their energy—and therefore ability to produce X-rays—after they leave the site where they were accelerated, the X-ray polarization probes the magnetic field geometry associated with the most efficient particle acceleration in the jet. One can therefore use measurements of the X-ray polarization, supplemented with contemporaneous multi-wavelength data, to infer the electron acceleration mechanism in blazar jets. Particle acceleration via shocks or magnetic reconnection is expected to be sufficiently efficient to cause the high-luminosity outbursts observed in blazars. In the former case, the magnetic field is partially ordered by the shock, leading to a high degree of polarization with the electric vector aligned with the jet axis (except for oblique shocks). Magnetic reconnection, on the other hand, can result in a polarization angle that depends on the orientation of the reconnection layer, which is unrelated to the jet direction except in special cases [10,11].

Another interesting question is the location of the emission region relative to the site where particle acceleration takes place. In the commonly invoked single-zone model, all of the emission originates in a single region with a uniform magnetic field. In this case, one expects a similar polarization degree and angle across frequencies. In a scenario characterized by multiple turbulent cells crossing a shock front [12], the mean degree of polarization, and its level of variability, should increase toward higher energies. This is caused by the number of emission zones with high enough electron energies to radiate above the synchrotron SED peak decreasing with frequency, thereby reducing the amount of incoherent averaging of the polarization vectors, e.g., [12,13]. The emission can also become energy-stratified as the electrons lose energy, owing to radiative cooling as they propagate downstream from the acceleration site [14]. In the energy-stratified model, we expect a much higher mean polarization toward higher frequencies [15,16].

The dominant X-ray emission process of "low-synchrotron-peaked" (LSP) blazars, whose SEDs peak below 10^{14} Hz, is less well established. A leading candidate is SSC or EC scattering, with low or essentially zero polarization expected [13,17,18]. If relativistic protons dominate the emission, the polarization degree is expected to be comparable to either the millimeter-radio or optical value, depending on whether the proton distribution is extended [19] or localized [20], respectively.

In what follows, we review the results of IXPE plus multi-wavelength observations that were published before 2024 July. This includes 16 IXPE observations of six HSP blazars, as well as more limited observations of LSP and ISP blazars and the radio galaxy Centaurus

A. The latter are mostly upper limits, which in some cases place meaningful constraints on the X-ray emission process.

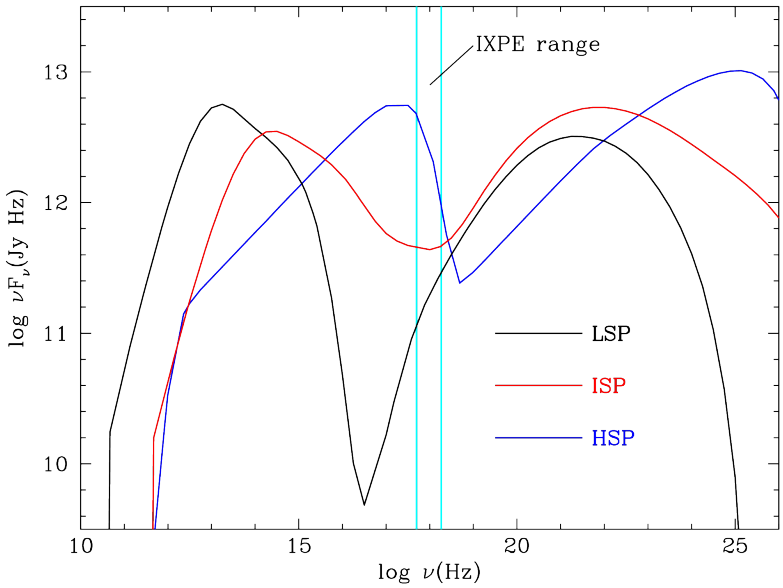

Figure 1. Sketch of the spectral energy distribution of a blazar for three different values of the peak frequency of the synchrotron emission.

Table 1. Contemporaneous X-ray and optical polarization of HSP blazars.

Object (Date)	**X-ray**		**Optical R-Band** [a]		**Jet PA(°) at 43 GHz** [b]
	$\Pi_X(\%)$	$\psi_X(°)$	$\Pi_O(\%)$	$\psi_O(°)$	
1ES0229 + 200 [c] (23 January 2023)	18 ± 3	$25 \pm 5°$	$2.4 \pm 0.7\%$	$2 \pm 8°$	163 ± 8
Mrk421 (5 May 2022)	$15 \pm 2\%$	35 ± 4	2.9 ± 0.5	32 ± 5	-29 ± 18
Mrk421 (5 June 2022)	10 ± 1	Rotation	4.4 ± 0.4	-40 ± 6	-29 ± 18
Mrk421 (8 June 2022)	10 ± 1	Rotation	5.4 ± 0.4	-35 ± 1	-29 ± 18
Mrk421 (17 December 2022)	14 ± 1	-73 ± 3	4.6 ± 1.3	26 ± 9	-29 ± 18
PG1553 + 113 (2 February 2023)	10 ± 2	86 ± 8	4.2 ± 0.5	Rotation	50 ± 10
Mrk501 (7 March 2022)	9.8 ± 1.7	136 ± 5	6.6 ± 0.4	110 ± 5	120 ± 12
Mrk501 (27 March 2022)	10.3 ± 1.4	115 ± 4	4.7 ± 0.3	120 ± 3	120 ± 12
Mrk501 (9 July 2022)	6.9 ± 1.8	134 ± 8	2.7 ± 0.5	109 ± 5	120 ± 12
Mrk501 (12 February 2023)	9.0 ± 2.4	110 ± 8	6.6 ± 0.9	150 ± 4	120 ± 12
Mrk501 (19 March 2023)	6.0 ± 2.1	107 ± 11	6.1 ± 0.7	125 ± 3	120 ± 12
Mrk501 (16 April 2023)	18.5 ± 2.2	103 ± 3	5.9 ± 1.5	108 ± 6	120 ± 12
1ES1959 + 650 (3 May 2022)	8.0 ± 2.3	123 ± 8	4.5 ± 0.2	159 ± 1	120–150
1ES1959 + 650 (10 June 2022)	< 5.1 [d]	—	4.7 ± 0.6	151 ± 19	120–150
1ES2155−304 (30 October 2023)	31 ± 2	129 ± 2	4.3 ± 0.7	116 ± 8	135 ± 45
1ES2155−304 (4 November 2023)	15 ± 2	125 ± 4	3.8 ± 0.9	116 ± 8	135 ± 45

Dates correspond to the middle of IXPE exposures. The values listed are compiled from 1ES0229 + 200 [21]; Mrk421 [22–24]; PG1553+113 [25]; Mrk501 [26–28]; 1ES1959 + 650 [29]; 1ES2155−304 [30]. [a] Median polarization properties during the IXPE observation. Optical degree of polarization is corrected for dilution by unpolarized starlight from the host galaxy. [b] Determined from VLBA images [31–33]; www.bu.edu/blazars/BEAM-ME.html (accessed on 1 June 2024). [c] While 1ES0229 + 200 is often considered to be an "extreme" HSP, its multi-wavelength polarization properties are similar to other HSPs. [d] When the 200 ks IXPE exposure is divided into four equal time bins, the third time bin yields a significant detection of $\Pi_X = 7.5 \pm 2.3\%$, $\psi_X = 127 \pm 9°$ [29].

2. Observational Results and Theoretical Interpretations

2.1. HSP Blazars

As listed in Table 1, IXPE has detected polarization in all six of the HSPs that it has observed. The degree of polarization Π_X ranges from below 5.1% to $31 \pm 2\%$ (in 1ES2155−304).

In two of the blazars, the X-ray EVPA ψ_X is closely aligned with the jet direction (PA): 120° (median value of ψ_X) vs. $120 \pm 12°$ PA in Mrk501, and 127° (median value) vs. $135 \pm 30°$ PA in 1ES2155−304 [30]. The relation between ψ_X and PA in the other four blazars is less clear. In 1ES1959 + 650 in 2022 May, $\psi_X = 123 \pm 8°$ (with a similar value obtained in a single 50 ks time bin in 2022 June; see Table 1), which is essentially the same as the jet direction of $128 \pm 13°$ measured several years earlier [33] and 2 years later (See www.bu.edu/blazars/VLBA_GLAST/1959.html, accessed on 1 June 2024). The jets of many HSP blazars are broad (tens of degrees [33,34]), and PA is variable in some, such as PG1553 + 113 [32] and 1ES1959 + 650. Further contemporaneous IXPE and VLBA observations of a number of HSP blazars are needed to determine how closely related ψ_X is to the jet direction.

The multiple IXPE measurements of Mrk421, Mrk501, 1ES1959 + 650, and 1ES2155−304 reveal significant variability in their X-ray polarization, superseding reports of nearly constant Π_X based on early IXPE observations [26]. The degree of polarization of Mrk501 ranges from 6% to 18%, while ψ_X fluctuates by ±17° in the jet direction. This is similar to the long-term behavior of the optical polarization [35]. In 1ES1959 + 650, Π_X varies from $\leq$5.1% to 12.4%, similar to, although somewhat stronger than, typical fluctuations in the optical polarization (See www.bu.edu/blazars/VLBA_GLAST/1959.html, accessed on 1 June 2024) . Between the first and second halves of a ∼10-day exposure of 1ES2155−304, IXPE measures Π_X to decline from 31% to 15%, while ψ_X remains steady within the uncertainties.

The degree of X-ray polarization in Mrk421, the brightest blazar at X-ray energies most of the time, varies more modestly, between 10% and 15%, but with quite dramatic variations of ψ_X, with no apparent relation to the jet direction. In June 2022 ψ_X rotated at a constant (to within the uncertainties) rate by ∼380°, while Π_X remained at $10 \pm 1\%$ [23]. Such rotations, which have been observed previously in blazars at optical wavelengths (e.g., ψ_O rotated by 125°, while ψ_X remained stable in PG1553 + 113; [25]), can be interpreted as the result of the motion of the emitting plasma (e.g., a shock or plasmoid) through a helical magnetic field, with the line of sight lying within the cone of the helix [23,36–38]. The helical field could reside in a "spine" of the jet, while longer-wavelength emission is mainly produced in a surrounding "sheath" [23]. EVPA rotations also could correspond to stochastic variations caused by turbulence [12,39]. However, statistics indicate that at least some of the observed rotations are non-stochastic [38]. If, as expected, the X-ray emission in HSP blazars arises from the most upstream sections of the jet, observations of ψ_X rotations can potentially probe the processes by which the jet is accelerated and collimated, as well as the particle acceleration mechanism.

The ratio $\langle \Pi_X / \Pi_O \rangle$ of the six HSP blazars (averaged over time for each object) ranges from 1.7 to 7.5. This implies that the emission regions are, at most, partially co-spatial, with the magnetic field of the optically emitting region being more disordered than that of the X-ray zone. A simple model divides the source into N turbulent cells, each with a uniform magnetic field of random orientation [9,12,39]. The degree of polarization $\Pi \sim 75 N^{-1/2}\%$; hence, the expected ratio is $\langle \Pi_X / \Pi_O \rangle \sim (N_O / N_X)^{1/2}$. Under this model, the observed values of the ratio correspond to ∼3 to 60 times as many cells emitting at optical wavelengths as the number that emit at X-ray energies.

Frequency stratification of the emission region naturally results from the higher energies of electrons needed for X-ray versus optical synchrotron radiation. X-ray emission must occur very close to the site of particle acceleration, beyond which the electrons lose energy, while the optical emission continues over a larger volume. One way by which such energy stratification can occur is in a shock, where electrons are accelerated at the front, then advect away from the front [14] as sketched in Figure 2. The magnetic field should

be predominantly parallel to the shock front [16], and therefore perpendicular to the jet axis (unless the shock is oblique [40,41]). This ordering of the field should diminish as the plasma propagates downstream from the shock front, causing the polarization to decrease in the larger optically emitting region [16]. If the plasma is turbulent prior to crossing the shock, the EVPA could fluctuate erratically about the direction of the jet [12]. It is also possible for the X-rays to be emitted in a "spine" of the jet, close to the axis, while the optical to radio emission is mainly from a slower surrounding "sheath" [42]. For the majority of the HSPs in Table 1, however, the optical polarization is roughly aligned with the jet direction, whereas high-frequency radio images show that it tends to be perpendicular to that direction (e.g., [43–45]).

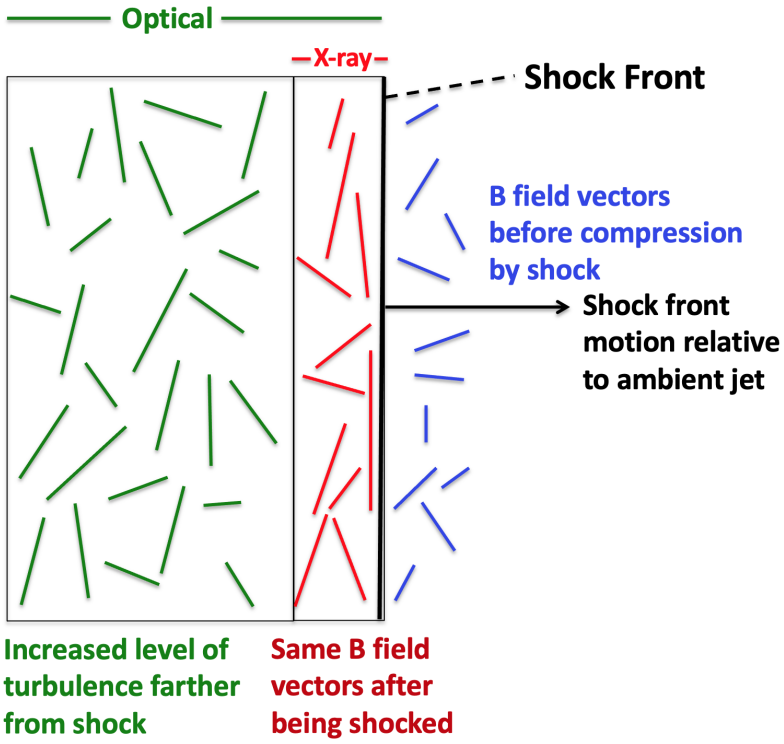

Figure 2. Sketch (not drawn to scale) of the structure of the magnetic field lines and frequency structure of turbulent plasma flowing across a shock front. The shock could be either stationary or moving down the jet.

Magnetic reconnection, e.g., [46] could also provide frequency stratification if particles are accelerated in localized sites and then lose energy as they stream away from those sites. If the reconnection occurs in a turbulent region, the EVPA would then be essentially random. Alternatively, if the opposing magnetic fields involved in reconnection correspond to reversals in the direction of a helical field permeating the jet, the EVPA could be parallel to the jet axis [16]. Further simulations of magnetic reconnection in relativistic jets are needed to determine whether the process naturally produces the frequency stratification that observations mandate.

The polarization properties of Mrk501 and 1ES2155-304 match the expectations of the shock model, with turbulence needed in Mrk501 to account for the fluctuations in EVPA in the jet direction. However, the wide difference in the two measurements ψ_X of Mrk421 when no EVPA rotation is observed corresponds better to magnetic reconnection in a turbulent plasma.

2.2. LSP and ISP Blazars

Among the non-HSP blazars observed by IXPE, which include the LSP-ISP BL Lacertae and ISP S5 0716+714, as well as the LSPs 3C 273, 3C 279, and 3C 454.3, only up-

per limits to the 2–8 keV polarization were obtained [47–49]. However, at one epoch, significant polarization ($\Pi_X = 21.7^{+5.6}_{-7.9}$%) was detected from BL Lac when constricting the energy range to 2–4 keV [48]. The optical polarization at that time was significantly lower, $\Pi_O = 13.1 \pm 2.4$%, while both the X-ray and optical EVPAs were $\sim 40^\circ$ from the jet axis. This conforms with the energy dependence of the polarization expected for an ISP, whose softer X-ray emission arises from synchrotron radiation, while the harder emission is from Compton scattering.

The X-ray upper limits, which range from 9% to 30%, eliminate models in which very high X-ray polarization is expected. These include proton synchrotron radiation and pair cascades following hadron–photon collisions [13]. Compton scattering remains a viable candidate for the X-ray emission mechanism.

2.3. Radio Galaxy Centaurus A

Centaurus A is the only radio galaxy observed by IXPE thus far, with the result being an upper limit of $\Pi_X \leq 6.5\%$ [50]. This is consistent with Compton scattering as the origin of the X-ray emission in the compact (sub-kiloparsec) regions of the jet. An analysis of the radio to X-ray polarized SED found that the data are consistent with frequency-stratified SSC, with the magnetic field transverse to the jet in the upstream regions (which can be associated with sites of particle acceleration) and parallel to the jet downstream as predicted in the shock model of [16].

3. Discussion

The strong X-ray polarization measured in the HSP blazars confirms the impression one obtains from the SED: the X-rays are produced by synchrotron radiation from the relativistic jet. Electrons radiating at such high frequencies must have very high energies, $\gtrsim$10 GeV, which requires efficient particle acceleration. The higher degree of X-ray versus optical polarization implies that the lower-frequency emission arises mostly from regions that are farther from the site of acceleration. This occurs naturally in shock models [14] but might also result from magnetic reconnection [46]. In either case, the plasma appears to be turbulent to account for time variations of the EVPA and its deviations from the jet direction [12,16]. Further polarization measurements of the same objects are needed to define the variability properties, and the continued development of models is required to generate firmer predictions of the polarization behavior. Contemporaneous very long baseline interferometry at millimeter wavelengths should be performed to determine the jet direction, which can change quite dramatically on time scales of months to years (e.g., [32,33,51,52]).

The X-ray EVPA rotation observed in Mrk421 [23] implies that some of the X-ray emission is produced by plasma propagating down regions of the jet where the magnetic field is helical. This is expected in the zone where the jet is accelerated to higher bulk Lorentz factors and collimated into a very narrow cone [53]. Observing such events for a longer time, as well as in different blazars, should allow a probe of this poorly explored region.

For the LSP blazars and radio galaxies, the current observations are consistent with Compton scattering as the origin of the X-ray emission. Actual detections, rather than upper limits, could confirm whether this is the case. For synchrotron self-Compton (SSC) radiation [2], the X-ray polarization should be $\sim$30–40% of the millimeter-wave and sub-millimeter-wave values [17], with similar EVPAs. The mean short-millimeter-wave linear polarization of all blazars in the POLAMI program is below 10% [54,55]; hence, the SSC model predicts $\Pi_X \lesssim 4\%$. If the seed photons are nearly unpolarized as expected for thermal sources, $\Pi_X \sim 0$ is expected [17]. Thus far, we have been limited by the relatively low X-ray flux of LSPs during the IXPE observations. The majority of LSP observations by IXPE have yielded upper limits of $\lesssim$14% or more [49]. Future observations of flaring LSPs can potentially decrease the upper limits. The detection of weak X-ray polarization during a very bright X-ray flare could differentiate between different Compton scattering models.

4. Conclusions

Measurements of X-ray polarization made possible by IXPE provide new information on the X-ray emission process and particle acceleration in the relativistic jets of RLAGNs. The results thus far confirm that the emission regions are energy-stratified. The observed properties of some HSP blazars match the predictions of models incorporating both shocks and turbulence. In others, the EVPAs appear not to agree with the basic shock scenario, leaving room for magnetic reconnection to be the driving force behind particle acceleration in those blazars. For LSP blazars and the radio galaxy Cen A, the upper limits to the degree of polarization are in accord with the X-ray emission from Compton scattering, but the detection of weak polarization in some of these objects, possibly during states of high X-ray flux (otherwise, long integration times risk the vector cancellation of the polarization if the EVPA varies [56]), would provide more definitive tests.

IXPE and multi-wavelength observations have therefore improved our knowledge of the physical processes operating in relativistic jets. Additional observations to explore further the temporal behavior of the X-ray and multi-wavelength emission of RLAGNs should continue to prove enlightening.

Author Contributions: A.P.M. wrote the first draft of the paper, while L.D.G., S.G.J., D.E.K., I.L., R.M. and F.T. contributed to the final version. All authors have read and agreed to the published version of the manuscript.

Funding: The Imaging X-ray Polarimetry Explorer (IXPE) is a joint US and Italian mission. The US contribution is supported by the National Aeronautics and Space Administration (NASA) and led and managed by its Marshall Space Flight Center (MSFC), with industry partner Ball Aerospace (contract NNM15AA18C). The Italian contribution is supported by the Italian Space Agency (Agenzia Spaziale Italiana, ASI) through contract ASI-OHBI-2017-12-I.0, agreements ASIINAF- 2017-12-H0 and ASI-INFN-2017.13-H0, and its Space Science Data Center (SSDC), and by the Istituto Nazionale di Astrofisica (INAF) and the Istituto Nazionale di Fisica Nucleare (INFN) in Italy. This research used data products provided by the IXPE Team (MSFC, SSDC, INAF, and INFN) and distributed with additional software tools by the High-Energy Astrophysics Science Archive Research Center (HEASARC), at NASA Goddard Space Flight Center (GSFC). The research of APM and SGJ was partially supported by National Science Foundation grant AST-2108622, NASA Swift grant 80NSSC23K1145, NASA NuSTAR grant 80NSSC22K0537, and NASA Fermi grant 80NSSC23K1507. RM acknowledges financial support from ASI-INAF agreement n. 2022-14-HH.0.

Data Availability Statement: The data used to compose Table 1 can be found in the sources cited in the table notes.

Acknowledgments: The VLBA is an instrument of the National Radio Astronomy Observatory. The National Radio Astronomy Observatory is a facility of the National Science Foundation operated under cooperative agreement by Associated Universities, Inc.

Conflicts of Interest: The authors declare no conflicts of interest.

Abbreviations

The following abbreviations are used in this manuscript:

IXPE	Imaging X-ray Polarimetry Explorer
HSP	High-synchrotron-peak blazar
ISP	Intermediate-synchrotron-peak blazar
LSP	Low-synchrotron-peak blazar

References

1. Haardt, F.; Maraschi, L. A Two-Phase Model for the X-ray Emission from Seyfert Galaxies. *Astrophys. J. Lett.* **1991**, *380*, L51. [CrossRef]
2. Jones, T.W.; O'Dell, S.L.; Stein, W.A. Physics of Compact Nonthermal Sources. I. Theory of Radiation Processes. *Astrophys. J.* **1974**, *188*, 353–368. [CrossRef]

3. Sikora, M.; Begelman, M.C.; Rees, M.J. Comptonization of Diffuse Ambient Radiation by a Relativistic Jet: The Source of Gamma Rays from Blazars? *Astrophys. J.* **1994**, *421*, 153. [CrossRef]
4. Böttcher, M.; Reimer, A.; Sweeney, K.; Prakash, A. Leptonic and Hadronic Modeling of Fermi-detected Blazars. *Astrophys. J.* **2013**, *768*, 54. [CrossRef]
5. Weisskopf, M.C.; Soffitta, P.; Baldini, L.; Ramsey, B.D.; O'Dell, S.L.; Romani, R.W.; Matt, G.; Deininger, W.D.; Baumgartner, W.H.; Bellazzini, R.; et al. The Imaging X-ray Polarimetry Explorer (IXPE): Pre-Launch. *J. Astron. Telesc. Instruments Syst.* **2022**, *8*, 026002. [CrossRef]
6. Weisskopf, M.C.; Elsner, R.F.; O'Dell, S.L. On understanding the figures of merit for detection and measurement of x-ray polarization. In Proceedings of the Space Telescopes and Instrumentation 2010: Ultraviolet to Gamma Ray, San Diego, CA, USA, 28 June–2 July 2010; Volume 7732, p. 77320E. [CrossRef]
7. Abdo, A.A.; Ackermann, M.; Agudo, I.; Ajello, M.; Aller, H.D.; Aller, M.F.; Angelakis, E.; Arkharov, A.A.; Axelsson, M.; Bach, U.; et al. The Spectral Energy Distribution of Fermi Bright Blazars. *Astrophys. J.* **2010**, *716*, 30–70. [CrossRef]
8. Lyutikov, M.; Pariev, V.I.; Gabuzda, D.C. Polarization and structure of relativistic parsec-scale AGN jets. *Mon. Not. R. Astron. Soc.* **2005**, *360*, 869–891. [CrossRef]
9. Burn, B.J. On the depolarization of discrete radio sources by Faraday dispersion. *Mon. Not. R. Astron. Soc.* **1966**, *133*, 67. [CrossRef]
10. Zhang, H.; Li, X.; Guo, F.; Giannios, D. Large-amplitude Blazar Polarization Angle Swing as a Signature of Magnetic Reconnection. *Astrophys. J. Lett.* **2018**, *862*, L25. [CrossRef]
11. Hosking, D.N.; Sironi, L. A First-principle Model for Polarization Swings during Reconnection-powered Flares. *Astrophys. J. Lett.* **2020**, *900*, L23. [CrossRef]
12. Marscher, A.P. Turbulent, Extreme Multi-zone Model for Simulating Flux and Polarization Variability in Blazars. *Astrophys. J.* **2014**, *780*, 87. [CrossRef]
13. Liodakis, I.; Peirson, A.L.; Romani, R.W. Prospects for Detecting X-ray Polarization in Blazar Jets. *Astrophys. J.* **2019**, *880*, 29. [CrossRef]
14. Marscher, A.P.; Gear, W.K. Models for high-frequency radio outbursts in extragalactic sources, with application to the early 1983 millimeter-to-infrared flare of 3C 273. *Astrophys. J.* **1985**, *298*, 114–127. [CrossRef]
15. Angelakis, E.; Hovatta, T.; Blinov, D.; Pavlidou, V.; Kiehlmann, S.; Myserlis, I.; Böttcher, M.; Mao, P.; Panopoulou, G.V.; Liodakis, I.; et al. RoboPol: The optical polarization of gamma-ray-loud and gamma-ray-quiet blazars. *Mon. Not. R. Astron. Soc.* **2016**, *463*, 3365–3380. [CrossRef]
16. Tavecchio, F.; Landoni, M.; Sironi, L.; Coppi, P. Probing dissipation mechanisms in BL Lac jets through X-ray polarimetry. *Mon. Not. R. Astron. Soc.* **2018**, *480*, 2872–2880. [CrossRef]
17. Krawczynski, H. The Polarization Properties of Inverse Compton Emission and Implications for Blazar Observations with the GEMS X-ray Polarimeter. *Astrophys. J.* **2012**, *744*, 30. [CrossRef]
18. Peirson, A.L.; Romani, R.W. The Polarization Behavior of Relativistic Synchrotron Self-Compton Jets. *Astrophys. J.* **2019**, *885*, 76. [CrossRef]
19. Zhang, H.; Böttcher, M.; Liodakis, I. Revisiting High-energy Polarization from Leptonic and Hadronic Blazar Scenarios. *Astrophys. J.* **2024**, *967*, 93. [CrossRef]
20. Zhang, H.; Böttcher, M. X-ray and Gamma-Ray Polarization in Leptonic and Hadronic Jet Models of Blazars. *Astrophys. J.* **2013**, *774*, 18. [CrossRef]
21. Ehlert, S.R.; Liodakis, I.; Middei, R.; Marscher, A.P.; Tavecchio, F.; Agudo, I.; Kouch, P.M.; Lindfors, E.; Nilsson, K.; Myserlis, I.; et al. X-ray Polarization of the BL Lacertae Type Blazar 1ES 0229+200. *Astrophys. J.* **2023**, *959*, 61. [CrossRef]
22. Di Gesu, L.; Donnarumma, I.; Tavecchio, F.; Agudo, I.; Barnounin, T.; Cibrario, N.; Di Lalla, N.; Di Marco, A.; Escudero, J.; Errando, M.; et al. The X-ray Polarization View of Mrk 421 in an Average Flux State as Observed by the Imaging X-ray Polarimetry Explorer. *Astrophys. J. Lett.* **2022**, *938*, L7. [CrossRef]
23. Di Gesu, L.; Marshall, H.L.; Ehlert, S.R.; Kim, D.E.; Donnarumma, I.; Tavecchio, F.; Liodakis, I.; Kiehlmann, S.; Agudo, I.; Jorstad, S.G.; et al. Discovery of X-ray polarization angle rotation in the jet from blazar Mrk 421. *Nat. Astron.* **2023**, *7*, 1245–1258. [CrossRef]
24. Kim, D.E.; Di Gesu, L.; Liodakis, I.; Marscher, A.P.; Jorstad, S.G.; Middei, R.; Marshall, H.L.; Pacciani, L.; Agudo, I.; Tavecchio, F.; et al. Magnetic field properties inside the jet of Mrk 421. Multiwavelength polarimetry, including the Imaging X-ray Polarimetry Explorer. *Astron. Astrophys.* **2024**, *681*, A12. [CrossRef]
25. Middei, R.; Perri, M.; Puccetti, S.; Liodakis, I.; Di Gesu, L.; Marscher, A.P.; Rodriguez Cavero, N.; Tavecchio, F.; Donnarumma, I.; Laurenti, M.; et al. IXPE and Multiwavelength Observations of Blazar PG 1553+113 Reveal an Orphan Optical Polarization Swing. *Astrophys. J. Lett.* **2023**, *953*, L28. [CrossRef]
26. Liodakis, I.; Marscher, A.P.; Agudo, I.; Berdyugin, A.V.; Bernardos, M.I.; Bonnoli, G.; Borman, G.A.; Casadio, C.; Casanova, V.; Cavazzuti, E.; et al. Polarized blazar X-rays imply particle acceleration in shocks. *Nature* **2022**, *611*, 677–681. [CrossRef] [PubMed]
27. Lisalda, L.; Gao, E.; Krawczynski, H.; Tavecchio, F.; Liodakis, I.; Gokus, A.; Rodriguez Cavaro, N.; Nowak, M.; Negro, M.; Middei, R.; et al. IXPE Observations of the Blazar Mrk 501 in 2022: A Multiwavelength View. *Mon. Not. R. Astron. Soc.* **2024**, *submitted*.

28. Chen, C.T.J.; Liodakis, I.; Middei, R.; Kim, D.E.; Gesu, L.; Marco, A.; Ehlert, S.R.; Errando, M.; Negro, M.; Jorstad, S.G.; et al. X-ray and multiwavelength polarization of Mrk 501 from 2022 to 2023. *Astrophys. J.* **2024**, *submitted*.
29. Errando, M.; Liodakis, I.; Marscher, A.P.; Marshall, H.L.; Middei, R.; Negro, M.; Peirson, A.L.; Perri, M.; Puccetti, S.; Rabinowitz, P.L.; et al. Detection of X-ray Polarization from the Blazar 1ES 1959+650 with the Imaging X-ray Polarimetry Explorer. *Astrophys. J.* **2024**, *963*, 5. [CrossRef]
30. Kouch, P.M.; Liodakis, I.; Middei, R.; Kim, D.E.; Tavecchio, F.; Marscher, A.P.; Marshall, H.L.; Ehlert, S.R.; Di Gesu, L.; Jorstad, S.G.; et al. IXPE observation of PKS 2155-304 reveals the most highly polarized blazar. *arXiv* **2024**, arXiv:2406.01693. [CrossRef]
31. Piner, B.G.; Edwards, P.G. Multi-epoch VLBA Imaging of 20 New TeV Blazars: Apparent Jet Speeds. *Astrophys. J.* **2018**, *853*, 68. [CrossRef]
32. Lico, R.; Liu, J.; Giroletti, M.; Orienti, M.; Gómez, J.L.; Piner, B.G.; MacDonald, N.R.; D'Ammando, F.; Fuentes, A. A parsec-scale wobbling jet in the high-synchrotron peaked blazar PG 1553+113. *Astron. Astrophys.* **2020**, *634*, A87. [CrossRef]
33. Weaver, Z.R.; Jorstad, S.G.; Marscher, A.P.; Morozova, D.A.; Troitsky, I.S.; Agudo, I.; Gómez, J.L.; Lähteenmäki, A.; Tammi, J.; Tornikoski, M. Kinematics of Parsec-scale Jets of Gamma-Ray Blazars at 43 GHz during 10 yr of the VLBA-BU-BLAZAR Program. *Astrophys. J.* **2022**, *260*, 12. [CrossRef]
34. Jorstad, S.G.; Marscher, A.P.; Lister, M.L.; Stirling, A.M.; Cawthorne, T.V.; Gear, W.K.; Gómez, J.L.; Stevens, J.A.; Smith, P.S.; Forster, J.R.; et al. Polarimetric Observations of 15 Active Galactic Nuclei at High Frequencies: Jet Kinematics from Bimonthly Monitoring with the Very Long Baseline Array. *Astron. J.* **2005**, *130*, 1418–1465. [CrossRef]
35. Marscher, A.P.; Jorstad, S.G. Linear Polarization Signatures of Particle Acceleration in High-Synchrotron-Peak Blazars. *Universe* **2022**, *8*, 644. [CrossRef]
36. Marscher, A.P.; Jorstad, S.G.; D'Arcangelo, F.D.; Smith, P.S.; Williams, G.G.; Larionov, V.M.; Oh, H.; Olmstead, A.R.; Aller, M.F.; Aller, H.D.; et al. The inner jet of an active galactic nucleus as revealed by a radio-to-γ-ray outburst. *Nature* **2008**, *452*, 966–969. [CrossRef] [PubMed]
37. Marscher, A.P.; Jorstad, S.G.; Larionov, V.M.; Aller, M.F.; Aller, H.D.; Lähteenmäki, A.; Agudo, I.; Smith, P.S.; Gurwell, M.; Hagen-Thorn, V.A.; et al. Probing the Inner Jet of the Quasar PKS 1510-089 with Multi-Waveband Monitoring During Strong Gamma-Ray Activity. *Astrophys. J. Lett.* **2010**, *710*, L126–L131. [CrossRef]
38. Blinov, D.; Pavlidou, V.; Papadakis, I.; Kiehlmann, S.; Liodakis, I.; Panopoulou, G.V.; Pearson, T.J.; Angelakis, E.; Baloković, M.; Hovatta, T.; et al. RoboPol: Do optical polarization rotations occur in all blazars? *Mon. Not. R. Astron. Soc.* **2016**, *462*, 1775–1785. [CrossRef]
39. Jones, T.W. Polarization as a Probe of magnetic Fields and Plasma Properties of Compact Radio Sources: Simulation of Relativistic Jets. *Astrophys. J.* **1988**, *332*, 678. [CrossRef]
40. Lind, K.R.; Blandford, R.D. Semidynamical models of radio jets: Relativistic beaming and source counts. *Astrophys. J.* **1985**, *295*, 358–367. [CrossRef]
41. Aller, H.D.; Aller, M.F.; Hughes, P.A. Magnetic Field Structures in Parsec Scale Jets: Oblique Shocks. In *Radio Astronomy at the Fringe*; Zensus, J.A., Cohen, M.H., Ros, E., Eds.; Astronomical Society of the Pacific Conference Series; Astronomical Society of the Pacific: San Francisco, CA, USA, 2003; Volume 300, p. 143.
42. Ghisellini, G.; Tavecchio, F.; Chiaberge, M. Structured jets in TeV BL Lac objects and radiogalaxies. Implications for the observed properties. *Astron. Astrophys.* **2005**, *432*, 401–410. [CrossRef]
43. Pushkarev, A.B.; Gabuzda, D.C.; Vetukhnovskaya, Y.N.; Yakimov, V.E. Spine-sheath polarization structures in four active galactic nuclei jets. *Mon. Not. R. Astron. Soc.* **2005**, *356*, 859–871. [CrossRef]
44. MacDonald, N.R.; Jorstad, S.G.; Marscher, A.P. "Orphan" γ-Ray Flares and Stationary Sheaths of Blazar Jets. *Astrophys. J.* **2017**, *850*, 87. [CrossRef]
45. Paraschos, G.F.; Debbrecht, L.C.; Kramer, J.A.; Traianou, E.; Liodakis, I.; Krichbaum, T.P.; Kim, J.Y.; Janssen, M.; Nair, D.G.; Savolainen, T.; et al. Evidence of a toroidal magnetic field in the core of 3C 84. *Astron. Astrophys.* **2024**, *686*, L5. [CrossRef]
46. Sironi, L.; Spitkovsky, A. Relativistic Reconnection: An Efficient Source of Non-thermal Particles. *Astrophys. J. Lett.* **2014**, *783*, L21. [CrossRef]
47. Middei, R.; Liodakis, I.; Perri, M.; Puccetti, S.; Cavazzuti, E.; Di Gesu, L.; Ehlert, S.R.; Madejski, G.; Marscher, A.P.; Marshall, H.L.; et al. X-ray Polarization Observations of BL Lacertae. *Astrophys. J. Lett.* **2023**, *942*, L10. [CrossRef]
48. Peirson, A.L.; Negro, M.; Liodakis, I.; Middei, R.; Kim, D.E.; Marscher, A.P.; Marshall, H.L.; Pacciani, L.; Romani, R.W.; Wu, K.; et al. X-ray Polarization of BL Lacertae in Outburst. *Astrophys. J. Lett.* **2023**, *948*, L25. [CrossRef]
49. Marshall, H.L.; Liodakis, I.; Marscher, A.P.; Di Lalla, N.; Jorstad, S.G.; Kim, D.E.; Middei, R.; Negro, M.; Omodei, N.; Peirson, A.L.; et al. Observations of Low and Intermediate Spectral Peak Blazars with the Imaging X-ray Polarimetry Explorer. *arXiv* **2023**, arXiv:2310.11510. [CrossRef]
50. Ehlert, S.R.; Ferrazzoli, R.; Marinucci, A.; Marshall, H.L.; Middei, R.; Pacciani, L.; Perri, M.; Petrucci, P.O.; Puccetti, S.; Barnouin, T.; et al. Limits on X-ray Polarization at the Core of Centaurus A as Observed with the Imaging X-ray Polarimetry Explorer. *Astrophys. J.* **2022**, *935*, 116. [CrossRef]
51. Agudo, I.; Marscher, A.P.; Jorstad, S.G.; Gómez, J.L.; Perucho, M.; Piner, B.G.; Rioja, M.; Dodson, R. Erratic Jet Wobbling in the BL Lacertae Object OJ287 Revealed by Sixteen Years of 7 mm VLBA Observations. *Astrophys. J.* **2012**, *747*, 63. [CrossRef]

52. Escudero Pedrosa, J.; Agudo, I.; Tramacere, A.; Marscher, A.P.; Jorstad, S.; Weaver, Z.R.; Casadio, C.; Thum, C.; Myserlis, I.; Fuentes, A.; et al. Repeating flaring activity of the blazar AO 0235+164. *Astron. Astrophys.* **2024**, *682*, A100. [CrossRef]
53. Vlahakis, N. Disk-Jet Connection. In *Blazar Variability Workshop II: Entering the GLAST Era*; Miller, H.R., Marshall, K., Webb, J.R., Aller, M.F., Eds.; Astronomical Society of the Pacific Conference Series; Astronomical Society of the Pacific: San Francisco, CA, USA, 2006; Volume 350, p. 169.
54. Agudo, I.; Thum, C.; Ramakrishnan, V.; Molina, S.N.; Casadio, C.; Gómez, J.L. POLAMI: Polarimetric Monitoring of Active Galactic Nuclei at Millimetre Wavelengths—III. Characterization of total flux density and polarization variability of relativistic jets. *Mon. Not. R. Astron. Soc.* **2018**, *473*, 1850–1867. [CrossRef]
55. Agudo, I.; Thum, C. The Polarized Emission of AGN at Millimeter Wavelengths as Seen by POLAMI. *Galaxies* **2022**, *10*, 87. [CrossRef]
56. Di Gesu, L.; Tavecchio, F.; Donnarumma, I.; Marscher, A.; Pesce-Rollins, M.; Landoni, M. Testing particle acceleration models for BL Lac jets with the Imaging X-ray Polarimetry Explorer. *Astron. Astrophys.* **2022**, *662*, A83. [CrossRef]